Structural and Mutational Studies of the Catalytic Domain of Colicin E5: A tRNA-Specific Ribonuclease[†,‡]

Yi-Lun Lin,[||] Youssef Elias,[§] and Raven H. Huang*[,§]

Department of Chemistry and Department of Biochemistry, University of Illinois, 600 South Mathews Avenue, Urbana, Illinois 61801

Received April 23, 2005; Revised Manuscript Received May 25, 2005

ABSTRACT: Colicin E5 specifically cleaves four tRNAs in *Escherichia coli* that contain the modified nucleotide queuosine (Q) at the wobble position, thereby preventing protein synthesis and ultimately resulting in cell death. Here, the crystal structure of the catalytic domain of colicin E5 (E5-CRD) from *E. coli* was determined at 1.5 Å resolution. Unexpectedly, E5-CRD adopts a core folding with a four-stranded β-sheet packed against an α-helix, seen in the well-studied ribonuclease T1 despite a lack of sequence similarity. Beyond the core catalytic domain, an N-terminal helix, a C-terminal β-strand and loop, and an extended internal loop constitute an RNA binding cleft. Mutational analysis identified five amino acids that were important for tRNA substrate binding and cleavage by E5-CRD. The structure, together with the mutational study, allows us to propose a model of colicin E5−tRNA interactions, suggesting the molecular basis of tRNA substrate recognition and the mechanism of tRNA cleavage by colicin E5.

The ribosome is the target for many protein toxins, including ricin (*1*), α-sarcin (*2*, *3*), and colicin E3 (*4*). Ricin carries out its toxic effect by depurinating A2660 (*Escherichia coli* numbering used throughout) of the 23S rRNA (*5*, *6*), while α-sarcin and colicin E3 cleave a specific phosphodiester bond in rRNA (the bond between G2661 and A2662 in 23S rRNA for α-sarcin and the bond between A1493 and G1494 in 16S rRNA for colicin E3) (*7*−*9*).

Less is known about protein toxins that target another essential component of protein synthesis, tRNAs. To date, three tRNA-specific toxins have been discovered (*10*). All of them are ribonucleases that cleave a phosphodiester bond in the anticodon region of a tRNA, yielding common RNA termini with a 2′,3′-cyclic phosphate and a 5′-OH group. PrrC, the first toxin of this class to be discovered, is a suicide device acquired by some *E. coli* strains when infected by T4 phage, resulting in cleavage of its own $tRNA^{lys}$ (5′-end of the wobble base) (*11*, *12*). Subsequently, two colicins from some *E. coli* strains were also shown to be tRNA-specific ribonucleases. Colicin D cleaves the phosphodiester bond between nucleotides 38 and 39 of $tRNA^{arg}$ (*13*). Colicin E5, the subject of this study, targets four tRNAs containing a hypermodified nucleotide Q[1] at the wobble position (position 34) and cleaves the phosphodiester bond between Q34 and U35 (*14*).

Except for colicin E1, which exerts its toxic effect by disrupting the membrane of the target cell through channel formation, E group colicins were thought to induce their toxic effect by either inhibiting DNA replication via deoxyribonuclease (DNase) activity or inhibiting protein biosynthesis via ribosomal ribonuclease (RNase) activity. Indeed, E2 and E7−E9 have been shown to have DNase activity, and E3, E4, and E6 have been shown to have ribosomal RNase activity. In support of the classification of E colicins into two subfamilies (DNase or RNase), members of each subfamily share sequence homology in the catalytic domain as well as their cognate immunity proteins. The only exception is colicin E5, which shares little sequence homology in the activity domain with members of either the DNase or RNase subfamily. The target of colicin E5 remained a mystery until Masaki and co-workers (*14*) showed that four tRNAs ($tRNA^{tyr}$, $tRNA^{his}$, $tRNA^{asn}$, and $tRNA^{asp}$), all possessing a hypermodified nucleotide Q at the wobble position, were cleaved at the phospodiester bond 3′-end of Q34 by colicin E5 (*14*).

Colicin E5 has particular interest based on the following observations. First, the catalytic domain of colicin E5 is unique in that it not only lacks sequence homology with the E group of colicins discussed above but also lacks sequence similarity with other known ribonucleases. Thus, the evolutionary origin of colicin E5 remains unknown. Second, colicin E5 is one of the only three tRNA-specific ribonucleases discovered to date, and it is the only colicin that targets a hypermodified nucleotide. This raises the questions of why a hypermodified nucleotide was targeted for recognition and how the modified nucleotide is recognized. Third, unlike many known ribonucleases, the catalytic domain of colicin E5 does not contain a single histidine, raising the question of how RNA cleavage is achieved without the involvement of histidine, as is required in other ribonucleases. Finally, the catalytic domain of colicin E5 has no sequence homology with tRNA guanine transglycosylase (TGT), the enzyme that is responsible for incorporation of the hypermodified nucleotide Q at the wobble position of the four

[†] This research was supported by a start-up fund from the University of Illinois at Urbana-Champaign and NIH Grant CA90954.

[‡] The coordinates for the structure have been deposited with the Protein Data Bank as entry 2A8K.

* To whom correspondence should be addressed. Phone: (217) 333-3967. Fax: (217) 244-5858. E-mail: huang@uiuc.edu.

[||] Department of Chemistry.

[§] Department of Biochemistry.

[1] Abbreviations: E5-CRD, E5 C-terminal region domain; Q, queuosine; PAGE, polyacrylamide gel electrophoresis; rmsd, root-mean-square deviation.

10.1021/bi050749s CCC: $30.25
Published on Web 07/16/2005

tRNAs. Thus, the structural analysis of colicin E5 provides a system for understanding the mechanisms by which two distinct enzymes recognize the same substrate.

We report here our biochemical and structural studies of E5-CRD, with an attempt to address some of issues described above. We found that, despite a lack of sequence similarity, E5-CRD adopted a similar fold seen in the toxin RelE, the catalytic domain of colicin D, and the ribonuclease T1, implying a common evolutionary origin. The structure of E5-CRD beyond the core domain, however, formed a unique cleft, accounting for its tRNA substrate recognition. Mutational analysis identified a pair of D/R amino acids that are likely to be involved in RNA cleavage, indicating that the presence of a histidine in the active site might not be a prerequisite for RNA cleavage. Structural comparison of E5-CRD reported here with tRNA guanine transglycosylase showed different approaches of molecular recognition of the same RNA substrate by these two enzymes.

MATERIALS AND METHODS

Cloning, Overexpression, and Purification of E5-CRD. The gene encoding both E5-CRD and its cognate immunity protein (ImmE5) was amplified by PCR from the ColE5-009 plasmid and was cloned into pLM-1 using SacI and HindIII restriction sites, thus generating a recombinant pLM-1-E5-CRD/ImmE5 plasmid. The gene starts with the 108th residue from the C-terminus of colicin E5 (Glu mutated to Met as the starting codon). Therefore, the resulting E5-CRD protein contains 108 amino acids, seven fewer than the one employed by Masaki and co-workers (*14*). The plasmids containing E5-CRD mutants were created by the QuickChange method using the recombinant pLM-1-E5-CRD/ImmE5 plasmid as the template. The plasmids were transformed into *E. coli* strain BL21(DE3). Wild-type and mutant proteins were overexpressed and purified to homogeneity. The purification procedures are similar to the ones used by Masaki and co-workers with minor modification (*14*).

RNA Cleavage Assays. All RNA cleavage experiments were performed at room temperature. RNA was radiolabeled with ^{32}P using T4 kinase and [γ-^{32}P]ATP (PE Science), and the radiolabeled RNA was purified with a Qiagen column. Unlabeled RNA was then added to the radiolabeled RNA to produce a final RNA concentration of 10 μM. A mixture of 10 nM E5-CRD, 2 μM RNA, and RNase inhibitor in 10 μL of buffer [100 mM NaCl, 20 mM Tris-HCl (pH 7.6), and 5 mM $MgCl_2$] was incubated at room temperature for 10 min. The reaction was stopped by addition of 10 μL of gel loading buffer and heating at 95 °C for 5 min. The sample was then loaded onto a 20% denaturing polyacrylamide gel. Electrophoresis was carried out in a 1× TBE buffer at 400 V for 3 h. The gel was dried and exposed to a phosphor screen (Fisher Scientific). Gel bands were visualized with a phosphorimager (Amersham Biosciences) and analyzed with ImageQuant (Molecular Dynamics, Sunnyvale, CA).

Crystallization, Data Collection, and Structural Determination. All crystals were obtained by the hanging-drop vapor diffusion method at 4 °C. Native crystals were grown against a well solution of 30% PEG400, 100 mM MES (pH 6.5), 100 mM NaCl, and 40 mM $CaCl_2$. Crystals of selenomethionine derivatives were grown against the same well solution with an exception that the concentration of PEG400 was elevated to 40%. Hexagonal crystals that diffracted to 1.5 Å resolution were obtained in 1 week. To carry out data collection at a low temperature, the crystals were first soaked in a cryo-protecting solution containing all the components of the well solution and 20% glycerol, mounted in a nylon loop, and then flash-frozen in liquid nitrogen. Both the native and three-wavelength anomalous dispersion (MAD) data were collected at beamline 14-BMC at Advanced Photon Source (APS). Data were reduced with Denzo and Scalepack (*15*). For phase determination, the resolution range from 30 to 2.0 Å was chosen. Four of four expected sites (assuming four molecules of E5-CRD in an asymmetric unit) were found using Solve (*16*). Phases were improved, and ~85% of the model was automatically built using Resolve (*17*). Several rounds of manual building using O (*18*), followed by refinement with CNS (*19*), resulted in a final model with an *R*-factor of 21.7% (R_{free} = 23.4%). Final refinement statistics are given in Table 1.

Table 1: Statistics of Data Collection and Refinement[a]

	inflection	peak	remote	native
data collection				
space group				$P3_1$
unit cell				65.22 Å, 65.22 Å, 100.74 Å, 90.00°, 90.00°, 120.00°
resolution (Å)	50.0−2.0	50.0−2.0	50.0−2.0	50.0−1.5
wavelength (Å)	0.9793	0.9791	0.9537	0.9793
no. of unique reflections	32043	32018	32141	76577
completeness (%)	99.2	99.2	99.4	99.8
average $I/\sigma(I)$[b]	9.2	9.9	9.8	21.3
redundancy	7.7	7.7	7.7	7.4
R_{sym}[c] (%)	6.5	6.6	7.3	3.5
refinement				
resolution (Å)				50.0−1.5
no. of reflections (free)				67751 (6027)
$R_{crystal}$[d] (R_{free}[e]) (%)				21.7 (23.4)
rmsd for bonds (Å)				0.0042
rmsd for angles (deg)				1.30

[a] Mean figure of merit (FOM) for phasing = 0.61 from SOLVE and 0.71 after RESOLVE. [b] $I/\sigma(I)$ is the mean reflection intensity/estimated error. [c] $R_{sym} = \sum|I - \langle I\rangle|/\sum I$, where I is the intensity of an individual reflection and $\langle I\rangle$ is the average intensity over symmetry equivalents. [d] $R_{crystal} = \sum||F_o| - |F_c||/\sum|F_o|$, where F_o and F_c are the observed and calculated structure factor amplitudes, respectively. [e] R_{free} is equivalent to $R_{crystal}$ but calculated for a randomly chosen set of reflections that were omitted from the refinement process.

Creation of E5-CRD Mutants and Assays of RNA Cleavage by These Mutants. Nineteen E5-CRD mutants (K13A, D15A, K17A, E24A, R25A, D46A, K47A, R48A, K51A, K52A, D56A, R60A, D62A, R79A, E82A, D88A, D96A, D97A, and R99A) were overexpressed and purified in a manner similar to that of wild-type E5-CRD. The initial RNA cleavage assays of these mutants were carried out under conditions identical to those described in RNA Cleavage Assays. It was found that D46A, R48A, K51A, D97A, and R99A mutations resulted in the severe reduction of the enzymatic activity of E5-CRD. Therefore, more detailed RNA cleavage assays of these mutants, together with the wild-type enzyme, in which the concentrations of the enzyme varied from 5 to 2000 nM, were carried out.

Construction of a Docking Model of the E5-CRD−RNA Complex. The structure of the anticodon stem−loop motif of $tRNA^{phe}$ (*20*) was employed to build a docking model.

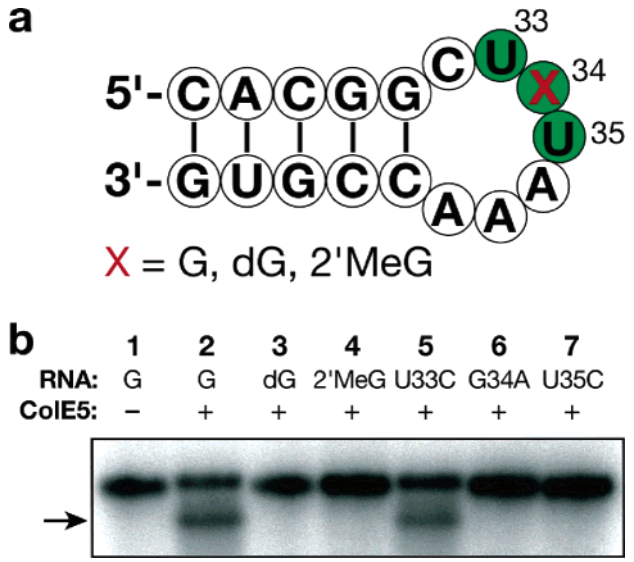

FIGURE 1: Cleavage of stem−loop RNAs with a natural or modified nucleotide at position 34 by E5-CRD. (a) Nucleotide sequence of stem−loop RNAs employed in this study. The conserved nucleotides required to be a substrate of colicin E5 are colored green. G represents guanosine, dG 2′-deoxyguanosine, and 2′MeG 2′-methoxyguanosine. (b) Denaturing PAGE analysis of the cleavage reactions. The bands indicated with an arrow are the cleavage products.

The nucleotide sequence of the anticodon was mutated from GAA to GUA using O (*18*). The G34 was then flipped out from the anticodon loop. The modified stem−loop RNA was then manually docked into the positively charged cleft in E5-CRD using PyMOL (*21*). It was necessary to adjust the conformation of U35 to accommodate the RNA molecule in the cleft of E5-CRD.

RESULTS AND DISCUSSION

Assays of RNA Cleavage by E5-CRD. To define the elements in the RNA substrate that are required for E5-CRD recognition and cleavage, a series of stem−loop RNAs, varying in the anticodon sequence, were prepared (Figure 1a). As it is not possible to prepare a stem−loop RNA with the modified nucleotide Q at position 34, the default stem−loop RNA substrate employed in our in vitro study contains a G at position 34 (Figure 1a, X = G). The radiolabeled stem−loop RNAs were incubated with purified E5-CRD, and resulting RNA cleavage products were analyzed by denaturing PAGE (Figure 1b). E5-CRD was able to cleave a stem−loop RNA with G at position 34 (Figure 1b, lane 2), consistent with the results reported by Masaki and co-workers (*14*). Replacement of G34 with a dG or a 2′MeG, however, resulted in resistance to cleavage of these RNAs by E5-CRD (lanes 3 and 4), indicating that the 2′-OH group in G34 plays an important role in RNA cleavage by E5-CRD. E5-CRD was able to cleave a stem−loop RNA in which U33 was replaced with a C, although at slightly lower efficiency (lane 5). Replacing G at position 34 with an A, however, significantly reduced or prevented cleavage of RNA by E5-CRD (lane 6). The same finding was observed for the U-to-C mutation at position 35 (lane 7). These results indicate that, at least for a G34-containing stem−loop RNA substrate and the catalytic domain of colicin E5, the recognition sequence in the RNA substrate is primarily G34 and U35 and, to a lesser extent, U33.

RNA cleavage assays were also performed in the presence or absence of divalent cations, such as Mg^{2+}, Mn^{2+}, and Ca^{2+}. E5-CRD cleaved the stem−loop RNA substrate equally well with or without divalent cations in the reaction mixture (data not shown), indicating that divalent cations such as Mg^{2+} are not involved in catalysis.

Structure of E5-CRD. The crystal structure of E5-CRD was determined using MAD phasing, and the structure was refined with several rounds of model building and simulated annealing. The asymmetric unit contains four molecules of E5-CRD, each consisting of residues 12−105. No electron density was observed for 11 and three residues at the N- and C-terminus, respectively, among which the N-terminal residues are part of a linker between the catalytic and receptor-binding domains of colicin E5.

The structure of E5-CRD is composed of two α-helices (α1 and α2, colored cyan in Figure 2a) and a five-stranded β-sheet (colored magenta in Figure 2a). The first four consecutive β-strands (β1−β4) run antiparallel, adjoined by the fifth and short C-terminal β-strand from the β1 side. N-Terminal helix α1 packs alongside β4, and the second helix, α2, packs over part of the β-sheet (β2−β4). The interactions between α-helices and the β-sheet are hydrophobic in nature. In addition to α-helices and β-strands, there are two long loops, located between β1 and β2 and between β4 and β5 (L1 and L2, respectively, Figure 2a). The structure of E5-CRD presented here is different from those of other E group colicins known to be nucleases (RNase or DNase), including E3 (*22*, *23*), E7 (*24*, *25*), and E9 (*26*). A Dali search (*27*) revealed no strong structural homology between E5-CRD and any known fold. However, several structures deposited in the Protein Data Bank do have weak structural homology with E5-CRD despite a lack of sequence similarity. These include the archaeal toxin RelE (PDB entry 1WMI; *Z* score = 3.7, rmsd = 3.5 Å) (*28*), the catalytic domain of colicin D (PDB entry 1V74; *Z* score = 3.5, rmsd = 2.7 Å) (*29*), and nuclease T1 (PDB entry 9RNT; *Z* score = 2.5, rmsd = 3.4 Å) (*30*). Interestingly, all three of these proteins are ribonucleases, which may imply a common evolutionary origin. The structure in common among these four proteins is the overall fold that encompasses a four-stranded β-sheet packed over an α-helix (β1−β4 and α2 shown in Figure 2a). This is a well-known fold for a superfamily of microbial ribonucleases, exemplified by nuclease T1 because of its extensive studies (Figure 2b). Beyond the core folding, the structures differ from one another (Figure 2b). In the case of E5-CRD, the N-terminal helix, internal loop (L1) from extended β1 and β2, and the C-terminus (including L2 and β5) constitute a unique cleft (Figure 2a) where the RNA substrate is predicted to bind (see below).

Four molecules of E5-CRD are present in the asymmetric unit, forming two pairs of tightly packed structures as shown in Figure 2c. The rmsd between these two pairs of packed structure is 0.1 Å, indicating that the structures of these two pairs are virtually identical. The rmsd between two monomers within the packed structure shown in Figure 2c is 1.7 Å. The difference is mainly caused by different conformations of the two C-terminal residues (residues 104 and 105). If these two residues are excluded during comparison, the rmsd improves to 1.0 Å. These structural comparisons indicate the overall structures of the four molecules in the asymmetric unit are essentially the same. The packing shown in Figure

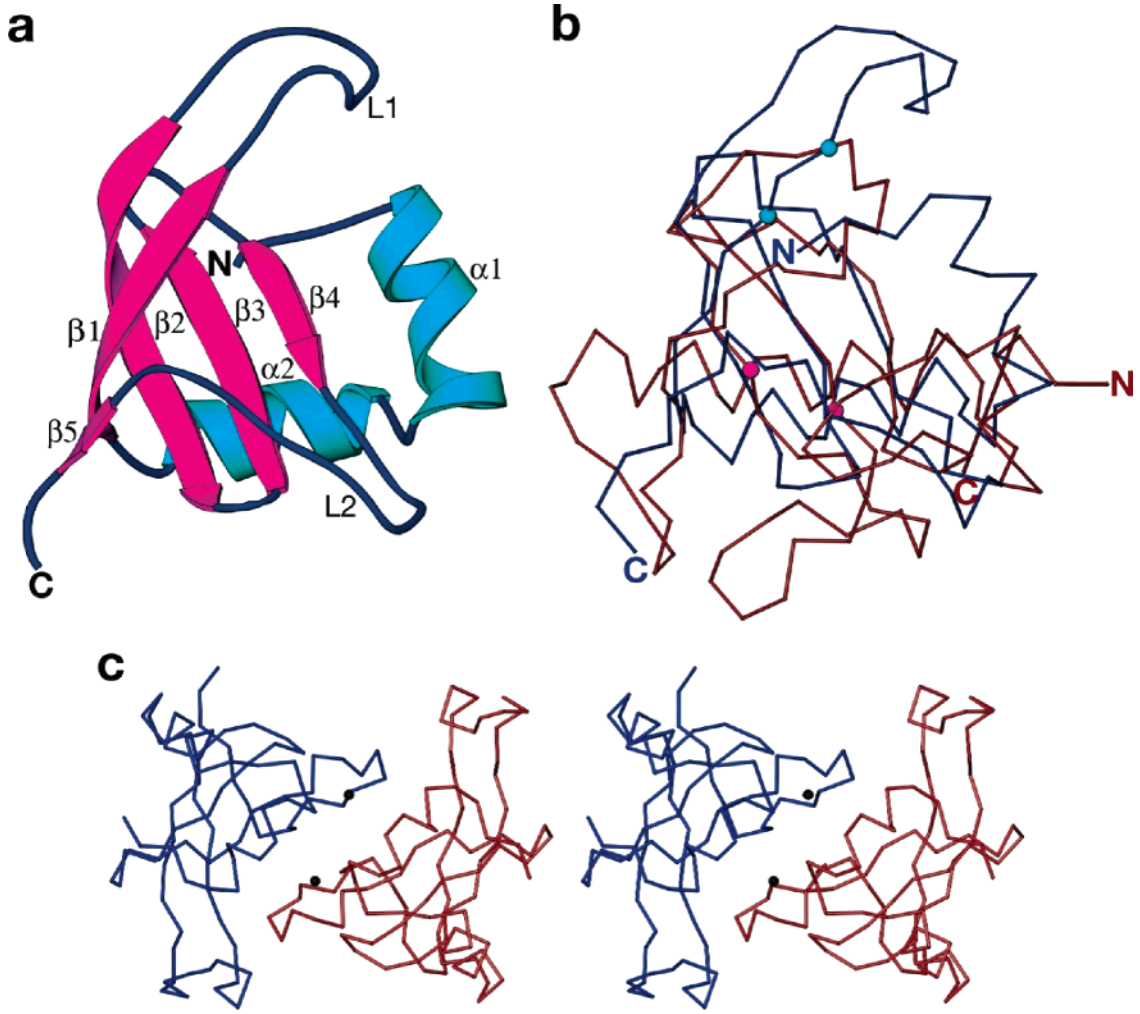

FIGURE 2: Structure of E5-CRD. (a) Ribbon representation of the E5-CRD. α-Helices are colored cyan, *β*-strands magenta, and coils grayish blue. (b) Cα superposition of E5-CRD (blue) with nuclease T1 (red, PDB entry 9RNT). The structures are in the same orientation as in panel a. The Cα atoms of the amino acids proposed to be responsible for RNA cleavage (D46 and R48 in E5-CRD and E58 and R77 in nuclease T1) are depicted as spheres, with the ones from E5-CRD in cyan and the ones from nuclease T1 in magenta. (c) Stereoview of two closed packed E5-CRD molecules in crystals (blue and red). The two calcium ions that contribute to the packing are depicted as black spheres.

2c results from the insertion of the negatively charged L2 of one molecule into the positively charged RNA binding cleft of the second molecule. In particular, two acidic residues in L2, D88 and D91, form salt bridges with the two basic residues, R25 and K17, in the RNA binding cleft, respectively. This interaction may be regarded as a mimic of RNA substrate binding. The packing is reinforced by an additional interaction between the N-terminal helices from both molecules, mediated by the side chains of E24 and T90 through two calcium ions. This accounts for the requirement of calcium ions in our crystallization solutions.

Mutational Analysis of Catalytic Activity. Although the shape of the cleft and its electrostatic nature (positive charge) suggested that the cleft may represent a site of RNA substrate binding, further mutagenesis studies were conducted to substantiate this possibility and to yield information about specific amino acids that may be responsible for recognition of G34 and U35, as well as catalysis. In deciding which residues to mutate, we relied on information from extensive studies on nuclease T1. It is generally believed that the conserved amino acid residues involved in catalysis in nuclease T1 are H40, E58, R77, and H92 (*31*). However, E5-CRD does not contain a histidine, and structural alignment of E5-CRD with nuclease T1 did not reveal the remaining equivalent amino acids (E58 and R77) in E5-CRD (Figure 2b). Nevertheless, we reasoned that such a pair of amino acids might also be required for colicin E5 to carry out the RNA cleavage reaction. Therefore, we performed an alanine scan of all acidic and basic residues (D, E, K, and R) that are located within or close to the RNA binding cleft, representing a total of 19 mutants. These mutants were overexpressed and purified, and RNA cleavage assays were carried out. Among the 19 mutants, 14 had minimal or no effect on RNA cleavage (Figure 3 and data not shown). Five mutants (D46A, R48A, K51A, D97A, and R99A), however, experienced significant reductions in their ability to cleave the stem−loop RNA substrate (Figure 3). For example, 8 nM wild-type E5-CRD was required to achieve 50% RNA cleavage (Figure 3, top panel), whereas each of these mutants at 400−800 nM was required to achieve the same level of RNA cleavage (Figure 3, panels 2−6). Therefore, mutation of these five amino acid residues resulted in a 50−100-fold reduction of the enzymatic activity of E5-CRD.

D46 and R48 are located in strand *β*1; K51 is located at the tip of loop L1, and D97 and R99 are located in loop L2. From a structural perspective, K51 is likely to be at the top

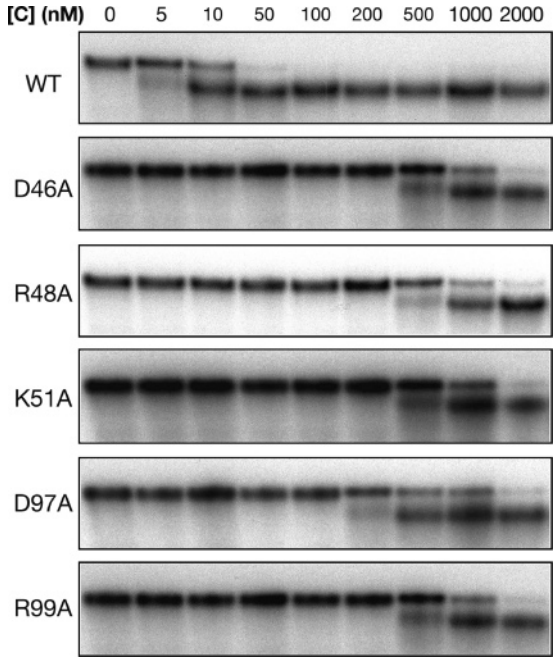

FIGURE 3: Efficiency of RNA cleavage by wild-type and mutated E5-CRD. The stem−loop RNA was incubated with increasing concentrations of the protein (marked on top) for 10 min at 25 °C, and the resulting samples were analyzed by denaturing PAGE.

of the RNA binding cleft, while the D46−R48 and D97−R99 pairs reside on two sides of the walls that form the cleft (Figure 4a). Therefore, their relative locations within the RNA binding cleft reveal their likely roles in terms of RNA substrate binding and cleavage, as discussed below.

Possible Recognition of RNA Substrate and Likely Mechanism of RNA Cleavage by E5-CRD. On the basis of the crystal structure of E5-CRD, together with the mutational study, a docking model of the RNA−protein complex was built (Figure 4b). The structure of the anticodon stem−loop portion of $tRNA^{phe}$ was manually docked into the positively charged cleft in E5-CRD (*20*). It was necessary to modify the conformation of G34 and U35, two recognition nucleotides, for docking without obvious steric constraints. In particular, targeted nucleotide G34 was flipped out. Generally, base flipping is regarded as a required mechanism for enzymes to catalyze chemical reactions on bases in DNA or RNA. For example, the most recent case includes RNA-modifying enzymes that catalyze modification reactions on nucleotides in the loop region of stem−loop RNAs (*32*, *33*). More importantly, the cocrystal structure of the restrictoxin−RNA complex shows a base flip mechanism for RNA substrate recognition and cleavage (*34*). Therefore, we believe that the RNA cleavage reaction carried out by E5-CRD is likely to be similar.

The docking model shows that the RNA substrate sits in a positively charged cleft of E5-CRD (Figure 4b, surface colored blue). The side chain of K51 is in the proximity of the phosphates of nucleotides 29 and 30 in RNA (Figure 4b). Therefore, the contribution of K51 to RNA binding is likely to be electrostatic. Targeted nucleotide G34 flips into a binding pocket. The pocket has sufficient space for the nucleotide of the natural substrate, Q, which is bulkier than G. Side chains of one of the critical D−R pairs in E5-CRD, D97 and R99, are near the base of G34, and are likely to be involved in molecular recognition of G34. Side chains of

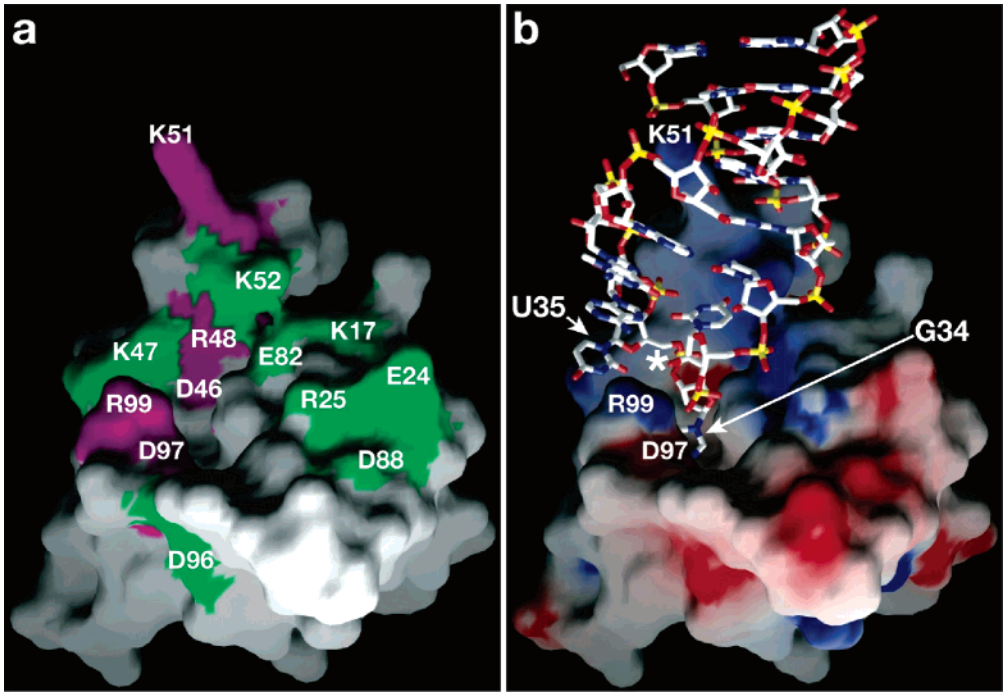

FIGURE 4: Surface representation of the structure of E5-CRD. (a) The data of the mutational analysis were mapped onto the structure of E5-CRD. The amino acids whose mutation resulted in a substantial reduction in activity are colored magenta, and the amino acids with a minor effect or no effect are colored green. Six additional mutants that have been mapped cannot be seen from this angle of structural display. (b) A docking model of the RNA−E5-CRD complex. E5-CRD is in the same orientation as in panel a except the surface is colored on the basis of electrostatic potential, with negative charge in red and positive charge in blue. The RNA is a stick and colored by individual atoms (white for carbon, blue for nitrogen, red for oxygen and yellow for phosphate). The scissile phosphodiester bond is marked with an asterisk.

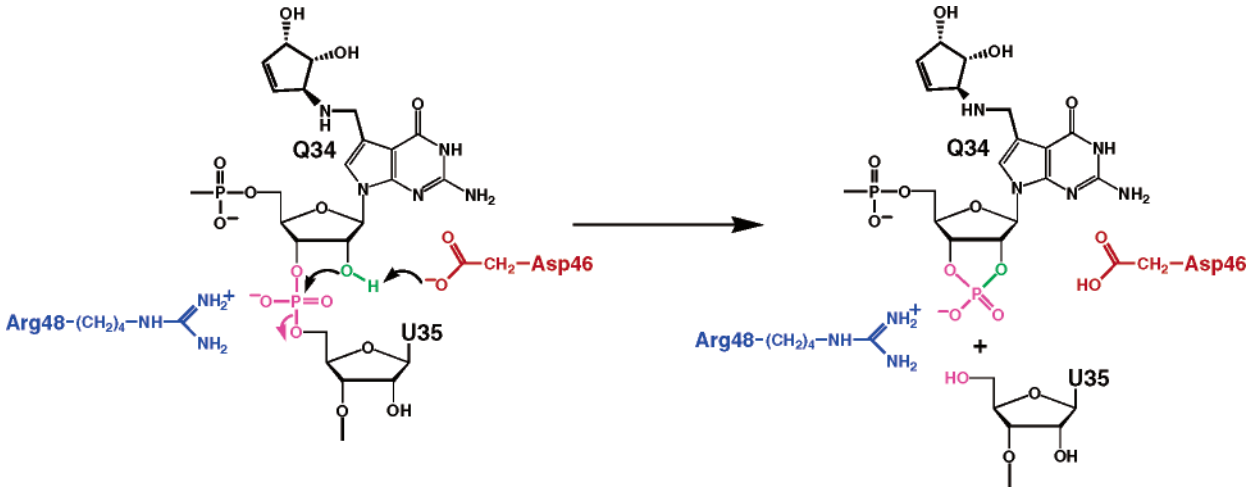

FIGURE 5: Proposed mechanism of RNA cleavage by colicin E5. Two critical amino acids, D46 (red) and R48 (blue), identified by the mutational study, are likely to be involved in catalysis. The 2′-OH group (green) of Q34 is the nucleophile that attacks the adjacent scissile phosphodiester bond (magenta), resulting in formation of the 2′,3′-cyclic phosphate in Q34 and the departure of the 5′-OH group of U35.

the second important D−R pair, D46 and R48, are near the scissile phosphodiester bond between G34 and U35 (marked with an asterisk in Figure 4b). Therefore, D46 and R48 are in positions to be directly involved in catalysis.

On the basis of these studies, a reasonable mechanism of tRNA cleavage by colicin E5 is proposed as shown in Figure 5. In this mechanism, the side chain of D46 acts as a general base, activating the 2′-OH group of the G34 to facilitate its nucleophilic attack on the adjacent phosphodiester bond. The transition state formed in the complex is likely to be stabilized by the side chain of R48. The roles of the D46−R48 pair in this proposed mechanism are thus similar to that of the E58−R77 pair in nuclease T1. We recognize that it is possible that amino acids other than D46 and R48 may also contribute to catalysis. Further mutational studies of amino acids surrounding the D46−R48 pair should reveal additional information in that regard. Ultimately, a crystal structure of the RNA−E5-CRD complex is required for confirmation of our hypothesis.

Concluding Remarks. Colicin E5 cleaves four tRNAs that contain a hypermodified nucleotide at the wobble position in a sequence-specific manner. The crystal structure of the catalytic domain of colicin E5 reveals that, although it adopts a core fold as seen in nuclease T1, it forms a cleft suitable for its tRNA substrate binding. The cleft is formed through the contribution of a N-terminal α-helix, an internal loop, and a C-terminal β-strand and a loop. The similar core folding with other microbial ribonucleases may imply that it has an evolutionary relationship with a more ancient microbial nuclease. However, to form a specific cleft for its strict recognition of Q-containing tRNA substrates, it has acquired extensive modifications through evolution. This may explain the fact that the catalytic domain of colicin E5 lacks sequence similarity with known ribonucleases. The lack of a histidine in the catalytic domain of colicin E5 seems at first surprising, considering that at least one histidine is involved in catalysis by many known ribonucleases that have been studied. However, as a toxin, colicin E5 only needs to "break" a tRNA molecule to make it unusable, and the minimum reaction is a transesterification reaction as depicted in Figure 5. Such a reaction, although perhaps more efficient when a histidine is involved, can be carried out with the involvement of only a D−R pair as proposed here on the basis of our mutational analysis. In contrast, nuclease T1 is involved in RNA metabolism. The transesterification reaction is only the first step of the reaction, which is followed by hydrolysis of the 2′,3′-cyclic phosphate, in which a histidine appears to be required (H92 in nuclease T1, H102 in barnase, and H119 in RNase A) (*31*, *35*, *36*).

ACKNOWLEDGMENT

We thank the staffs of beamline 14-BMC at APS (K. Brister, N. Lei, and R. Pahl) for their support during data collection. We also thank Dr. D. Brunner for the ColE5-099 plasmid and D. Kranz for helpful discussions and critical reading of the manuscript.

REFERENCES

1. Stillmark, H. (1888) in *Inaugural Dissertation*, Dorpat, Estonia.
2. Olson, B. H., and Goerner, G. L. (1965) Alpha Sarcin, a New Antitumor Agent. I. Isolation, Purification, Chemical Composition, and the Identity of a New Amino Acid, *Appl. Microbiol. 13*, 314−21.
3. Jennings, J. C., Olson, B. H., Roga, V., Junek, A. J., and Schuurmans, D. M. (1965) Alpha Sarcin, a New Antitumor Agent. II. Fermentation and Antitumor Spectrum, *Appl. Microbiol. 13*, 322−6.
4. James, R., Kleanthous, C., and Moore, G. R. (1996) The biology of E colicins: Paradigms and paradoxes, *Microbiology 142* (Part 7), 1569−80.
5. Endo, Y., Mitsui, K., Motizuki, M., and Tsurugi, K. (1987) The mechanism of action of ricin and related toxic lectins on eukaryotic ribosomes. The site and the characteristics of the modification in 28S ribosomal RNA caused by the toxins, *J. Biol. Chem. 262*, 5908−12.
6. Endo, Y., and Tsurugi, K. (1987) RNA N-glycosidase activity of ricin A-chain. Mechanism of action of the toxic lectin ricin on eukaryotic ribosomes, *J. Biol. Chem. 262*, 8128−30.
7. Endo, Y., and Wool, I. G. (1982) The site of action of α-sarcin on eukaryotic ribosomes. The sequence at the α-sarcin cleavage site in 28S ribosomal ribonucleic acid, *J. Biol. Chem. 257*, 9054−60.
8. Bowman, C. M., Dahlberg, J. E., Ikemura, T., Konisky, J., and Nomura, M. (1971) Specific inactivation of 16S ribosomal RNA induced by colicin E3 in vivo, *Proc. Natl. Acad. Sci. U.S.A. 68*, 964−8.
9. Senior, B. W., and Holland, I. B. (1971) Effect of colicin E3 upon the 30S ribosomal subunit of *Escherichia coli*, *Proc. Natl. Acad. Sci. U.S.A. 68*, 959−63.

10. Masaki, H., and Ogawa, T. (2002) The modes of action of colicins E5 and D, and related cytotoxic tRNases, *Biochimie 84*, 433−8.
11. Depew, R. E., and Cozzarelli, N. R. (1974) Genetics and physiology of bacteriophage T4 3′-phosphatase: Evidence for involvement of the enzyme in T4 DNA metabolism, *J. Virol. 13*, 888−97.
12. Kaufmann, G. (2000) Anticodon nucleases, *Trends Biochem. Sci. 25*, 70−4.
13. Tomita, K., Ogawa, T., Uozumi, T., Watanabe, K., and Masaki, H. (2000) A cytotoxic ribonuclease which specifically cleaves four isoaccepting arginine tRNAs at their anticodon loops, *Proc. Natl. Acad. Sci. U.S.A. 97*, 8278−83.
14. Ogawa, T., Tomita, K., Ueda, T., Watanabe, K., Uozumi, T., and Masaki, H. (1999) A cytotoxic ribonuclease targeting specific transfer RNA anticodons, *Science 283*, 2097−100.
15. Otwinowski, Z., and Minor, W. (1997) Processing of X-ray diffraction data collected in oscillation mode, in *Methods in Enzymology*, pp 307−26, Academic Press, San Diego.
16. Terwilliger, T. C., and Berendzen, J. (1999) Automated MAD and MIR structure solution, *Acta Crystallogr. D55* (Part 4), 849−61.
17. Terwilliger, T. C. (1999) Reciprocal-space solvent flattening, *Acta Crystallogr. D55*, 1863−71.
18. Jones, T. A., Zou, J.-Y., Cowan, S. W., and Kjeldgaard, M. (1991) Improved methods for building protein models in electron density maps and the location of errors in these models, *Acta Crystallogr. A47*, 110−9.
19. Brünger, A. T., Adams, P. D., Clore, G. M., DeLano, W. L., Gros, P., Grosse-Kunstleve, R. W., Jiang, J.-S., Kuszewski, J., Nilges, M., Pannu, N. S., Read, R. J., Rice, L. M., Simonson, T., and Warren, G. L. (1998) Crystallography & NMR System: A New Software Suite for Macromolecular Structure Determination, *Acta Crystallogr. D54*, 905−21.
20. Shi, H., and Moore, P. B. (2000) The crystal structure of yeast phenylalanine tRNA at 1.93 Å resolution: A classic structure revisited, *RNA 6*, 1091−105.
21. DeLano, W. L. (2002) *The PyMOL Molecular Graphic System*, DeLano Scientific, South San Francisco, CA.
22. Carr, S., Walker, D., James, R., Kleanthous, C., and Hemmings, A. M. (2000) Inhibition of a ribosome-inactivating ribonuclease: The crystal structure of the cytotoxic domain of colicin E3 in complex with its immunity protein, *Struct. Folding Des. 8*, 949−60.
23. Soelaiman, S., Jakes, K., Wu, N., Li, C., and Shoham, M. (2001) Crystal structure of colicin E3: Implications for cell entry and ribosome inactivation, *Mol. Cell 8*, 1053−62.
24. Ko, T. P., Liao, C. C., Ku, W. Y., Chak, K. F., and Yuan, H. S. (1999) The crystal structure of the DNase domain of colicin E7 in complex with its inhibitor Im7 protein, *Struct. Folding Des. 7*, 91−102.
25. Hsia, K. C., Chak, K. F., Liang, P. H., Cheng, Y. S., Ku, W. Y., and Yuan, H. S. (2004) DNA binding and degradation by the HNH protein ColE7, *Structure 12*, 205−14.
26. Kleanthous, C., Kuhlmann, U. C., Pommer, A. J., Ferguson, N., Radford, S. E., Moore, G. R., James, R., and Hemmings, A. M. (1999) Structural and mechanistic basis of immunity toward endonuclease colicins, *Nat. Struct. Biol. 6*, 243−52.
27. Holm, L., and Sander, C. (1993) Protein structure comparison by alignment of distance matrices, *J. Mol. Biol. 233*, 123−38.
28. Takagi, H., Kakuta, Y., Okada, T., Yao, M., Tanaka, I., and Kimura, M. (2005) Crystal structure of archaeal toxin-antitoxin RelE-RelB complex with implications for toxin activity and antitoxin effects, *Nat. Struct. Mol. Biol*. (in press).
29. Graille, M., Mora, L., Buckingham, R. H., Van Tilbeurgh, H., and De Zamaroczy, M. (2004) Structural inhibition of the colicin D tRNase by the tRNA-mimicking immunity protein, *EMBO J. 23*, 1474−82.
30. Martinez-Oyanedel, J., Choe, H. W., Heinemann, U., and Saenger, W. (1991) Ribonuclease T1 with free recognition and catalytic site: Crystal structure analysis at 1.5 Å resolution, *J. Mol. Biol. 222*, 335−52.
31. Steyaert, J. (1997) A decade of protein engineering on ribonuclease T1: Atomic dissection of the enzyme−substrate interactions, *Eur. J. Biochem. 247*, 1−11.
32. Hoang, C., and Ferre-D'Amare, A. R. (2001) Cocrystal structure of a tRNA ψ55 pseudouridine synthase: Nucleotide flipping by an RNA-modifying enzyme, *Cell 107*, 929−39.
33. Xie, W., Liu, X., and Huang, R. H. (2003) Chemical trapping and crystal structure of a catalytic tRNA guanine transglycosylase covalent intermediate, *Nat. Struct. Biol. 10*, 781−8.
34. Yang, X., Gerczei, T., Glover, L. T., and Correll, C. C. (2001) Crystal structures of restrictocin-inhibitor complexes with implications for RNA recognition and base flipping, *Nat. Struct. Biol. 8*, 968−73.
35. Schreiber, G., Frisch, C., and Fersht, A. R. (1997) The role of Glu73 of barnase in catalysis and the binding of barstar, *J. Mol. Biol. 270*, 111−22.
36. Thompson, J. E., and Raines, R. T. (1994) Value of general acid−base catalysis to ribonuclease A, *J. Am. Chem. Soc. 116*, 5467−8.

BI050749S